Design and first simulations of the TASEC-Lab power subsystem

S. Marín-Coca, D. González-Bárcena, S. Pindado and E. Roibás-Millán

Instituto Universitario de Mircrogravedad "Ignacio Da Riva" (IDR/UPM), ETSI Aeronáutica y del Espacio, Universidad Politécnica de Madrid, Spain

E-mail: sergio.marin.coca@upm.es, david.gonzalez@upm.es, santiago.pindado@upm.es and elena.roibas@upm.es

Abstract. This paper describes the modelling and simulation of the Electrical Power Subsystem (EPS) of the Thermal Analysis Support and Environment Characterization Laboratory (TASEC-Lab). TASEC-Lab is a university experiment on board a sub-orbital platform. It is designed to measure the convection heat transfer in high-altitude balloon missions. The EPS provides, regulates, and distributes electric power to the different systems, parts, and sensors that compose the TASEC-Lab (e.g., On Board Computer (OBC), temperature and pressure sensors, cup anemometer, GPS, heaters...). It mainly consists of a Li-ion battery and two DC-DC converters, and they have been characterized by conducting laboratory tests and fitting to experimental data. A real power consumption profile of the first TASEC-Lab's mission (designed by Universidad Politécnica de Madrid) is used as input to simulate the EPS. The mathematical model is validated by comparison with experimental results.

1. Introduction

The TASEC-Lab project consists of a university experiment that has been recently flown (July 2021) in a stratospheric balloon (see Figure 1a). Its main objective is to characterize the convective heat transfer on board this kind of platforms, which are becoming a very recurrent solution for testing technologies before going to space. The environmental conditions above 20 km (which are very similar to those in space) together with the economical advantages and the possibility of recovering the payload after the flight, make these platforms a suitable way to this purpose. However, they are not only used as testing platforms, but also as scientific platforms themselves. Many missions have been launched on board stratospheric balloons to study the Earth, the atmosphere, or even the Sun [1, 2]. Being above 99% of the atmosphere and having a constant view of the Sun makes these flights attractive to the scientific community.

The *Instituto Universitario de Microgravedad "Ignacio Da Riva"* (IDR/UPM Institute) has participated in the SUNRISE mission since its first flight in 2008. Staff from the IDR/UPM Institute have been responsible for the thermal control system and they have been in in charge of the thermal design and analysis [3]. Their work during these years arises some limitations when modelling the convective heat transfer during the flight, which motivates the analysis of this phenomenon using stratospheric balloon platforms. This kind of missions are usually analysed as space mission does. Although at the floating altitude the conductive and radiative heat

transfer are the main heat transfer mechanisms, the convective heat transfer is not negligible in some parts under certain conditions [4, 5].

TASEC-Lab has been designed for studying the convective heat transfer in high-altitude balloon missions, in order to obtain new correlations which will allow the thermal engineers to improve their models [6]. As responsible for the Master's Degree in Space Systems of the UPM, the IDR/UPM Institute decided to make TASEC-Lab a university project by involving Bachelor, Master and PhD students. The experiment has been completely designed, integrated, and tested by these students at the IDR/UPM Institute facilities. The development process of this experiment has been similar to the one involved in a satellite mission, following the same phases but using Commercial Of The Shelf (COTS) components to get a low cost design.

The mission concept proposed by B2Space (the company in charge of the gondola design and the operation of the launch) was to get an autonomous experiment in terms of electrical power. For that reason, the Electrical Power Subsystem (EPS) of TASEC-Lab experiment is one of the most important subsystems. It is responsible for providing and distributing the electrical power using only a battery as the main power supply. The flight was expected to last up to 8 hours, so no additional power source would be needed. However, a Power Control and Distribution Unit (PCDU) is required to provide the power to the different equipments on board.

Detailing the power budget of the system for sizing the battery is not enough for achieving a good design of the EPS. In this project, based on the expertise of the IDR/UPM Institute in this field [7–22], a numerical simulator of the EPS has been developed by conducting laboratory tests and fitting analytical models to experimental data. Modelling the behaviour of the DC-DC converters and the battery allows the simulation of the battery output voltage as well as the dissipated power in the DC-DC converters.

The work included in this paper describes how the EPS of TASEC-Lab has been designed, simulated, and tested. TASEC-Lab Power Subsystem is described in Section 2, and the modelling of the different components are detailed in Section 3. This model has been validated based on an estimated power profile as described in Section 3. Finally, Conclusions are summarized in Section 4.

2. TASEC-Lab EPS design

TASEC-Lab power subsystem (see Figure 1b), is designed with two main power lines with its own voltage level requirements. One line supplies power at 5 V to the On Board Computer (OBC), a Raspberry Pi 3B+. The OBC, in turn, feeds secondary power lines at 5 V and 3.3 V. The second main line is powered at 12 V and supplies power to the cup anemometer, its heater, and the experiment heater.

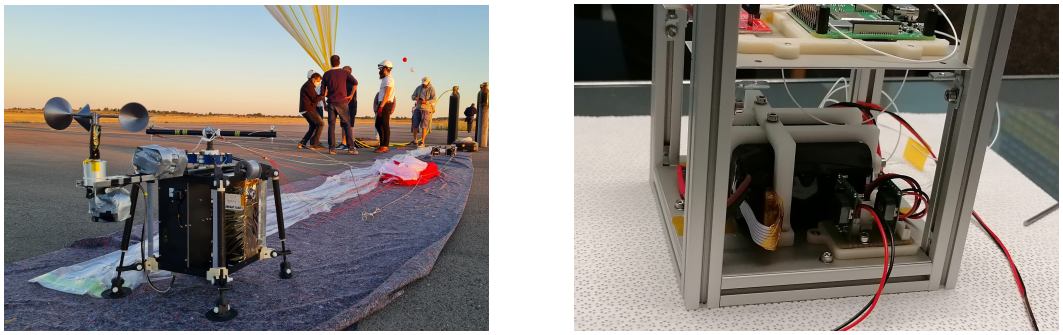

(a) (b)

Figure 1: TASEC-Lab during the pre-launch activities (a) and integration of the TASEC-Lab EPS (b).

The EPS is composed by a Li-ion battery, two DC-DC converters, a distribution harness, and a mechanical switch to turn on the system (see Figure 2). As the main power lines have different input voltages, and the voltage level of the battery changes with its State Of Charge (SOC), a DC-DC converter per line is needed. The selected DC-DC converters are compact and highly efficient buck converters [23]. Additionally, to ensure a good margin of remaining energy after the TASEC-Lab missions, the EPS carries a 24 V 2900 mA·h Samsung Li-ion battery [24]. Regarding the mechanical switch, it is made through a D-SUB-9 connector, which is attached to the lower tray and it is connected in series to the EPS bus line. To turn on the system, the anemometer would be connected from the outside closing the circuit between the battery and the DC-DC converters. This connector also allows the operation of the experiment without the anemometer during the tests or the battery charging.

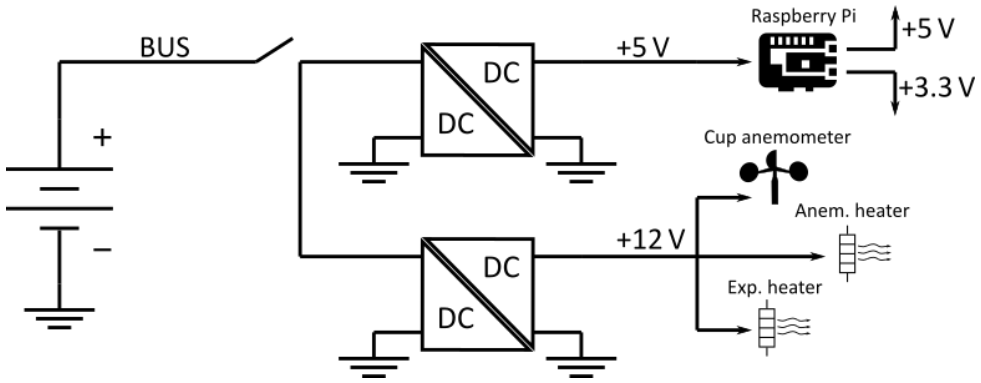

Figure 2: TASEC-Lab power subsystem simplified electrical circuit.

3. TASEC-Lab EPS modelling

The modelling of the EPS is an essential phase of the project. On the one hand, it helps to ensure that the battery is well-sized to supply enough power during the mission. On the other hand, the power losses affect the thermal behaviour of TASEC-Lab.

Several electrical and thermal tests have been performed emulating the electrical consumptions and thermal environment of the first TASEC-Lab flight, respectively. Additionally, TASEC-Lab is expected to perform additional flights, and the following missions or even the payloads can vary from one to another. For this reason, an EPS model is essential to predict the electrical and thermal behaviour of TASEC-Lab in future missions.

The EPS modelling starts analyzing the power consumption of the 5 V and 12 V lines. This is done by defining the operative modes of TASEC-Lab, which consists in detailing for each power line which components are turned on and its consumption at any time of the mission. An estimation of the power consumption of TASEC-Lab is shown in Figure 3. The next step is modelling the DC-DC converters. This allows to estimate their power losses, so the battery consumption can be predicted. Finally, it is necessary to model the discharging performance of the battery to predict its voltage or SOC during its operation. This is fundamental to determine if the battery is capable of supplying enough energy without exceeding safe margins of remaining capacity.

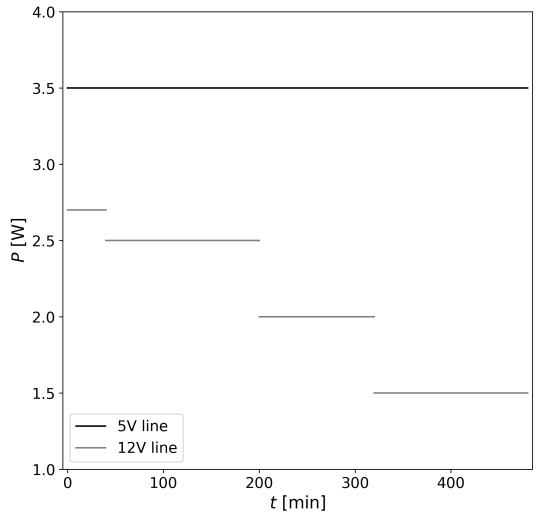

Figure 3: Estimated power consumption on the 5 V and 12 V line during the TASEC-Lab first mission (July 2021).

3.1. DC-DC converters

TASEC-Lab EPS carries the *R-78T5* and *R-78T12* DC-DC converters. Their datasheets [23] include their efficiency curves as a function of the output current for different input voltages. In the case of the *R-78T5* model (5 V output) these voltages are 42, 36, 24, 12 and 8 V, whereas the data of *R-78T12* model (12 V output) is presented for 42, 36, 24, and 15 V input voltage levels. Since the converters are connected in parallel to the battery, whose nominal voltage is around 22 V, the authors found compulsory an accurate characterization of the converters operating at this voltage.

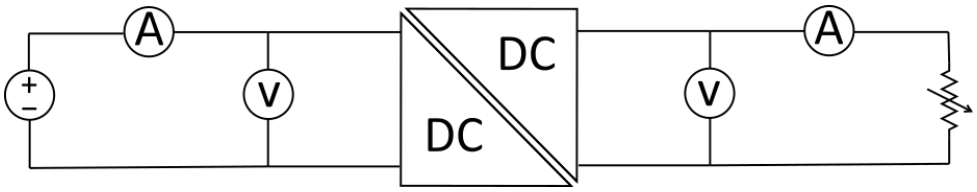

Figure 4: DC-DC converter electrical scheme test.

For this purpose, both DC-DC converters were tested following the the electrical circuit shown in Figure 4. This electrical circuit consists of one DC power source, four multimeters, an electronic load, and a DC-DC converter. This configuration allows an accurate measurement of the input and output voltages and currents of the DC-DC converters.

On the one hand, the power source provides an input voltage to the converter. The power source used is the *ISO-TECH IPS 3303* [25]. To increase the accuracy of the measured input current (I_{in}) and voltage (V_{in}), one multimeter is connected in series and another one in parallel. The first one is used as ammeter and the second acts as voltmeter. Both multimeters used are the *Promax PD-181* [26]. On the other hand, the electronic load is used to set the current consumption of the converter and the one used is the *Mayuno M9812* [27]. Two multimeters are connected at the DC-DC converter output to precisely measure the current (I_{out}) and the

voltage (V_{out}). Again, one in parallel acting as a voltmeter and the other in series with the electronic load used as an ammeter.

During the tests, the power source was supplying a constant voltage (measured by the input voltmeter) of 22 V. Moreover, the electronic load was configured to demand a current (measured with the ampermeter) from the minimum (0.1 A) to the maximum (1 A) output current in steps of 0.05 A. In total, 19 measurements of input and output current and voltage were collected for each of the two DC-DC converters. To give a graphical overview of the tests, the efficiencies of the converters were calculated according to Eq. 1. Then, these efficiencies were plotted as a function of the output current and for each input voltage (see Figure 5).

$$\eta = \frac{V_{out} I_{out}}{V_{in} I_{in}} \ . \tag{1}$$

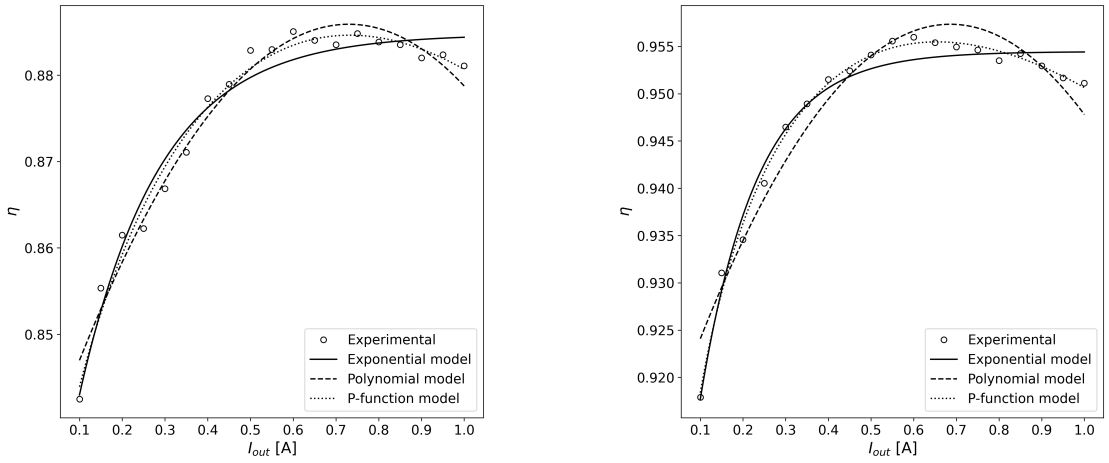

(a) Efficiency of the 5 V DC-DC converter.

(b) Efficiency of the 12 V DC-DC converter.

Figure 5: Efficiency of the DC-DC converters as a function of the output current for an input voltage of 22 V. The fitting curves are plotted with solid lines and the experimental data with cirlces.

According to Figure 5, the efficiency of both DC-DC converters rapidly increases with the current until it reaches a maximum, and then a quasilinear decrease is followed. In view of the results, the authors have characterized this behaviour with three models.

The first model, hereinafter *Exponential model*, is based on a previous work of the IDR/UPM Institute [7, 8]. In this model, the efficiency is defined as:

$$\eta\left(I_{out}\right) = \eta_{max}\left(1 - \exp\left(-\frac{I_{out}}{I_{ch}}\right)\right) \ , \tag{2}$$

where η_{max} is the maximum efficiency of the converter and I_{ch} is a characteristic current. In this case, this equation only partially describes the efficiency of the converter if it is slightly modified with the addition of the parameter I_0:

$$\eta\left(I_{out}\right) = \eta_{max}\left(1 - \exp\left(-\frac{I_{out} + I_0}{I_{ch}}\right)\right) \ . \tag{3}$$

The exponential model fits well the efficiency of the converters at low current outputs. However, for currents higher than the 50% of the maximum load, the fitting curve deviates (see Figure 5). The fitting parameters are presented in Table 1a.

A second model to better describe the efficiency at high output currents is proposed. This model, hereinafter *Polynomial model*, is represented by the following quadratic function:

$$\eta\left(I_{out}\right) = a{I_{out}}^2 + bI_{out} + c\ . \tag{4}$$

This second model fits well for almost the entire I_{out} (see Figure 5), but a, b and c parameters (see Table 1b) have no physical meaning.

Lastly, a third model consisting of a power function with a rational exponent has been developed. In this model, hereinafter *P-function model*, the efficiency is calculated as:

$$\eta\left(I_{out}\right) = \alpha{I_{out}}^{\beta} + \gamma I_{out} + \delta\ . \tag{5}$$

The *P-function model* fits the experimental data with precision (see Figure 5) and its parameters are shown in Table 1c.

Table 1: Fitting parameters of the DC-DC converters for an input voltage of 22 V.

(a) Exponential model.

	η_{max}	I_{ch} [A]	I_0 [A]
DC-DC$_{5V}$	0.8847	0.1886	0.4760
DC-DC$_{12V}$	0.9545	0.1330	0.3332

(b) Polynomial model.

	a [A^{-2}]	b [A^{-1}]	c [A]
DC-DC$_{5\ V}$	-0.0981	0.1432	0.8337
DC-DC$_{12\ V}$	-0.0969	0.1329	0.9118

(c) P-function model.

	α [A^{-1}]	β	γ [A^{-1}]	δ [A]
DC-DC$_{5\ V}$	1.6152	0.9413	-1.5483	0.8138
DC-DC$_{12\ V}$	0.2352	0.3183	$-$-0.0999	0.8153

To compare the precision of the developed converter efficiency models, the Root-Mean-Square Error (RMSE) of the efficiency has been calculated (see Table 2). Based on these results, the *P-function model* is selected to model the converters as it presents the lower value of RMSE.

Table 2: Root-Mean-Square Error (RMSE) of the proposed DC-DC converter efficiency models for an input voltage of 22 V.

	$\text{RMSE}_{\text{Exp. model}}$	$\text{RMSE}_{\text{Poly. model}}$	$\text{RMSE}_{\text{P-function model}}$
DC-DC$_{5\ V}$	$4.7855 \cdot 10^{-6}$	$3.5497 \cdot 10^{-6}$	$2.3104 \cdot 10^{-6}$
DC-DC$_{12\ V}$	$2.7807 \cdot 10^{-6}$	$5.3045 \cdot 10^{-6}$	$6.6284 \cdot 10^{-7}$

3.2. Battery

The selected battery has a nominal capacity of 2900 mA·h. In other words, the battery lasts 1 h being discharged at 2.9 A. However, TASEC-Lab is designed to operate several hours and the demanded current is variable with time. For that reason, battery discharge tests were performed to characterize its behaviour at different discharge rates.

A total of four battery discharging tests were carried on using the *Mayuno M9812* electronic load controlled by *Mayuno M9711* software. Starting from 25.2 V of Open Circuit Voltage

(OCV), and setting a cut-off voltage of 16.2 V, the battery was discharged at a constant rate of 1C, 0.5C, 0.25C and 0.1C (i.e., 2.9 A, 1.45 A, 0.745 A and 0.29 A). During the tests, the battery voltage, current, and elapsed time was measured and recorded.

The test data were used to characterize the battery with the linear discharging model based on the energy discharge level developed at the IDR/UPM Institute [12, 28]. In this model, the voltage level of the battery only depends on the the discharging current and the discharged energy, ϕ, defined as follows:

$$\phi(t) = \phi_0 + \int_{t_0}^{t} \left(VI + RI^2\right) \mathrm{d}t \ , \tag{6}$$

where V is the battery voltage, I the discharging current, R the internal resistance and ϕ_0 the initial discharged energy. In turn, the battery voltage is equal to OCV, $E(\phi)$, minus the voltage drop across the internal resistance:

$$V(\phi, I) = E(\phi) - RI \ . \tag{7}$$

In this model, the OCV only depends on the amount of discharged energy. In a first approach, if the battery is not fully discharged, $E(\phi)$ can be approximated by the following linear equation:

$$E(\phi) = E_0 + E_1\phi \ . \tag{8}$$

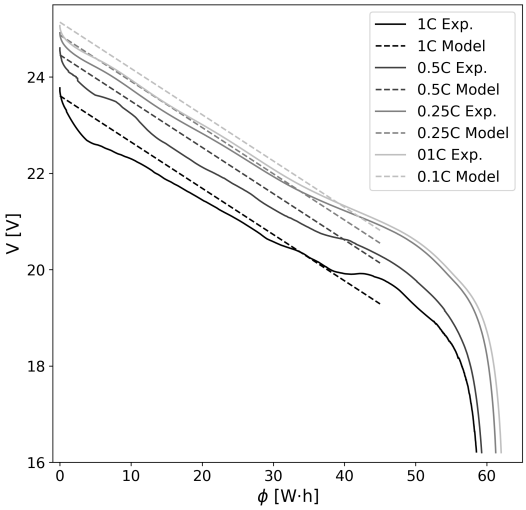

Figure 6: Evolution of the battery voltage, V, as a function of the discharged energy, ϕ, for different discharging current rates. Experimental results are plotted with solid lines and the fitting curves with dashed lines.

In Figure 6, the battery voltage as a function of the discharged energy, calculated with the experimental measurements and obtained with the proposed model, for different discharging current rates is shown. The parameters of the model (see Table 3) have been extracted by minimizing simultaneously the RMSE of the four experimental discharging curves. Moreover, the fidelity of the model is confirmed by the small values of RMSE presented in Table 4. It should be remarked that this model is valid as long as the discharging energy does not exceed

around 45 W·h. Additionally, the lower discharging current, the better precision of the model. These two conditions are met in the TASEC-Lab mission, as shown in the following section. Therefore, its possible to conclude that the selected model is appropriate for the EPS modelling.

Table 3: Parameters of the battery discharging model.

E_0 [V]	E_1 [$\frac{\text{V}}{\text{W·h}}$]	R [Ω]
25.307	$-9.6052 \cdot 10^{-2}$	$5.8541 \cdot 10^{-1}$

Table 4: Voltage root-mean-square deviation (RMSE) of the battery discharging model for different discharging current rates.

	RMSE
1C	$8.5305 \cdot 10^{-2}$
0.5C	$8.7933 \cdot 10^{-2}$
0.25C	$2.5770 \cdot 10^{-2}$
0.1C	$3.9354 \cdot 10^{-2}$

4. Simulation and model validation

TASEC-Lab has been tested with the estimated power profile of its first mission. Besides, the experimental results have been compared with a simulation to validate the proposed model. The power consumption profile, shown in Figure 3, is decomposed in the two secondary power lines. The 5 V line consumes a constant power of 3.5 W and the 12 V line presents four intervals of different constant consumption. The consumptions of the 5 V and 12 V lines are emulated with the *IT8512A Programmable DC Electronic Load* [29] and the *BK Precision 8500 Programable Electronic Load* [30], respectively. On the other hand, the battery voltage is measured with the aforementioned *Mayuno M9812*. The electrical circuit of the test is shown in Figure 7.

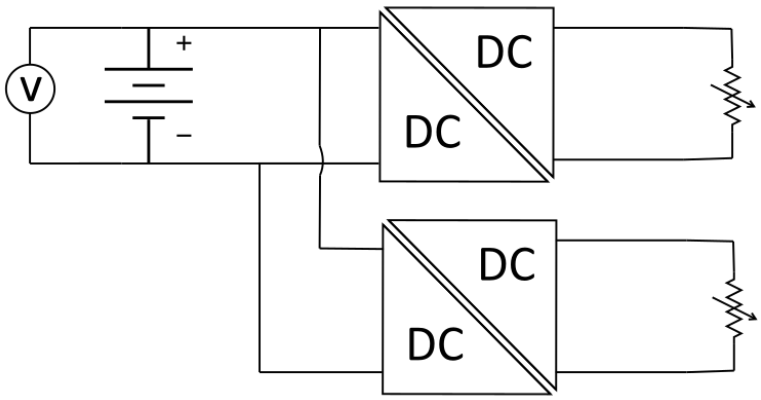

Figure 7: TASEC-Lab electrical circuit test.

On the other hand, the simulation is carried out coupling the performance of the DC-DC converters and the battery with the following equation:

$$P(t) = \frac{P_{5\mathrm{V}}}{\eta_{5\mathrm{V}}} + \frac{P_{12\mathrm{V}}(t)}{\eta_{12\mathrm{V}}(t)} \ , \tag{9}$$

where $P(t)$ is the battery power consumption, $P_{5\mathrm{V}}$ and $P_{12\mathrm{V}}$ are the demanded power on the 5 V and 12 V lines and $\eta_{5\mathrm{V}}$, $\eta_{12\mathrm{V}}$ are the efficiencies of the converters providing 5 V and 12 V as output. Then, the following differential equation is solved:

$$\frac{\mathrm{d}\phi}{\mathrm{d}t} = P + RI^2 \ , \tag{10}$$

where the discharging current, I, is calculated as:

$$I = \frac{P}{V} \ , \tag{11}$$

and the initial condition is:

$$\phi(t = 0) = 0 \ . \tag{12}$$

From this simulation, the most important results are shown in Figures 8 and 9. In Figure 8a the evolution of the converters efficiency is shown. The efficiency of the 5 V converter is constant during the whole simulation as expected, since the output current remains constant. As for the 12 V converter, its efficiency decreases in constant intervals likewise its output current. Moreover, in Figure 8b the evolution of the bus current and the lines that supply power to the converters is shown. The input current to the 5 V converter (line 1) linearly increases with time, since the power consumption of this converter remains constant but the battery voltage decreases with time. Regarding the input current of the 12 V converter (line 2), decreases with a saw tooth shape, as the converter power consumption decreases in constant intervals. As for the bus current is just the addition of the currents from lines 1 and 2.

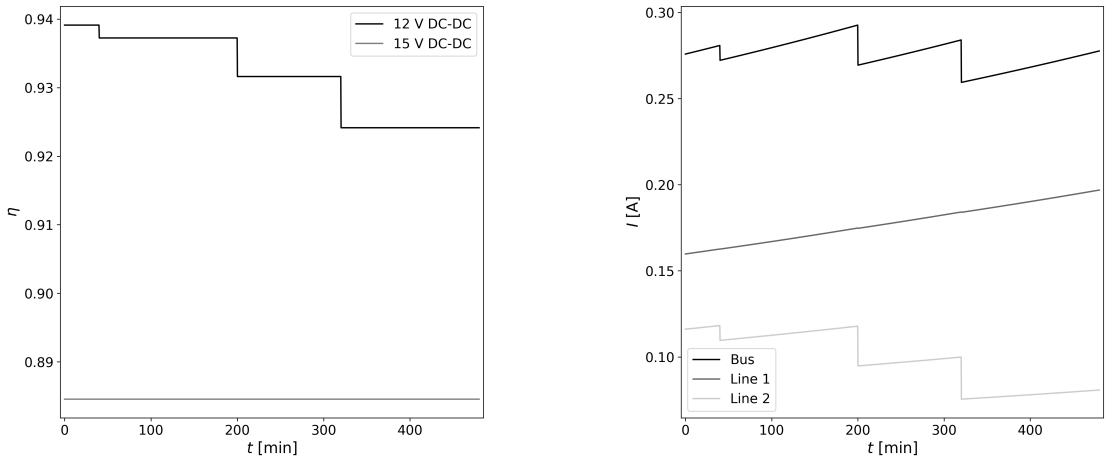

(a) (b)

Figure 8: Evolution of the converters efficiency (a) and the current through the bus and the power lines 1 and 2 (b) during the simulation.

Finally, the evolution of the battery voltage extracted from the experimental measurements and from the simulation is shown in Figure 9. According to this figure, the behaviour of the

simulated discharging curve is similar to the experimental one in the first third of the mission time. Then the simulated voltage starts to deviate from the measured voltage until reaches a maximum error of approximately 0.5 V. Regarding the modeling of TASEC-Lab EPS, these deviations are acceptable, since the relative error is lower than 3%.

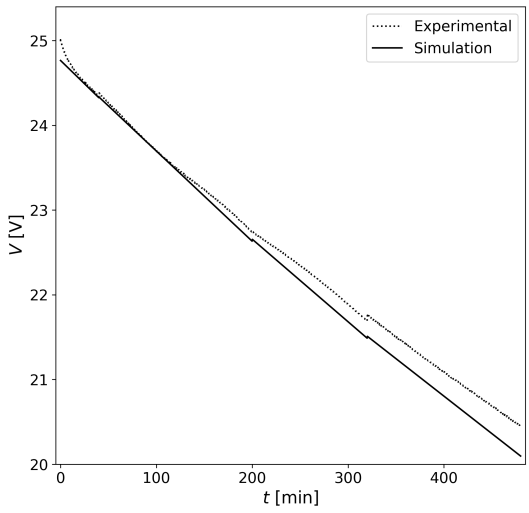

Figure 9: Evolution of the battery voltage during the test (dotted line) and the simulation (solid line).

5. Conclusion

The purpose of the current study was to model the power subsytem of the university experiment TASEC-Lab. Laboratory tests have been performed to model the behavior of the battery, the DC-DC converters, and the complete power system. The DC-DC model proposed in this paper (which is an original contribution), can accurately predict the performance of the converters and is innovative to the authors' knowledge. Additionally, the battery model developed at the IDR/UPM Institute presents a good fidelity with the experimental results. Finally, power subsystem simulations of further missions of TASEC-Lab will be carried out with the help of these models.

Acknowledgments

The authors are grateful for the support of the IDR/UPM Institute staff and the students from UPM involved in TASEC-Lab project.

References

[1] Barthol P, Gandorfer A, Solanki S K, Schüssler M, Chares B, Curdt W, Deutsch W, Feller A, Germerott D, Grauf B *et al.* 2011 *Solar Physics* **268** 1–34

[2] Solanki S, Riethmüller T, Barthol P, Danilovic S, Deutsch W, Doerr H P, Feller A, Gandorfer A, Germerott D, Gizon L *et al.* 2017 *The Astrophysical Journal Supplement Series* **229** 2

[3] Pérez-Grande I, Sanz-Andrés A, Bezdenejnykh N, Farrahi A, Barthol P and Meller R 2011 *Proceedings of the Institution of Mechanical Engineers, Part G: Journal of Aerospace Engineering* **225** 1037–1049

[4] González-Llana A, González-Bárcena D, Pérez-Grande I and Sanz-Andrés Á 2018 *Acta Astronautica* **148** ISSN 00945765

[5] González-Bárcena D, Fernández-Soler A, Pérez-Grande I and Sanz-Andrés Á 2020 *Acta Astronautica* ISSN 00945765

[6] Pérez L P, Ayape F, Martín J, González-Bárcena D and Muntean V 12-14 July 2021 *50th International Conference on Environmental Systems*

[7] Pindado, S and Roibás-Millán, E and Cubas, J and Álvarez, J M and Alfonso-Corcuera, D and Cubero-Estalrrich, J L and Gonzalez-Estrada, A and Sanabria-Pinzón, M, and Jado-Puente, R 2021 *IEEE Transactions on Industry Applications* **57** 1779–1788

[8] Porras-Hermoso, Ángel and Cobo-Lopez, B and Cubas, J and Pindado, S 2021 *Acta Astronautica* **179** 345–358

[9] Álvarez J M, Alfonso-Corcuera D, Roibás-Millán E, Cubas J, Cubero-Estalrrich J, Gonzalez-Estrada A, Jado-Puente R, Sanabria-Pinzón M and Pindado S 2021 *Applied Sciences* **11** ISSN 2076-3417 URL https://www.mdpi.com/2076-3417/11/9/4250

[10] Porras-Hermoso A, Cobo-Lopez B, Cubas J and Pindado S 2021 *Acta Astronautica* **179** 345–358 ISSN 0094-5765 URL https://www.sciencedirect.com/science/article/pii/S0094576520306317

[11] Zaragoza-Asensio J A, Pindado S and Pérez-Álvarez J 2021 *The Egyptian Journal of Remote Sensing and Space Science* **24** 311–317 ISSN 1110-9823 URL https://www.sciencedirect.com/science/article/pii/S1110982320303537

[12] Pindado S, Álvarez J M, Roibás-Millán E, Alfonso-Corcuera D, Cubas J and Gomez-San-Juan A M 2021 *IEEE Transactions on Industry Applications* **57** 3969–3977

[13] Gomez-San-Juan A M, Cubas J and Pindado S 2021 *IEEE Transactions on Aerospace and Electronic Systems* **57** 1672–1684

[14] Roibás-Millán E, Alfonso-Corcuera D, Cubas J, Álvarez J M, Pindado S and Gomez-San-Juan A M 2020 Performance analysis of photovoltaic systems: research at idr/upm institute *2020 IEEE International Conference on Environment and Electrical Engineering and 2020 IEEE Industrial and Commercial Power Systems Europe (EEEIC / I CPS Europe)* pp 1–6

[15] Roibás-Millán E, Cubero-Estalrrich J L, Gonzalez-Estrada A, Jado-Puente R, Sanabria-Pinzón M, Alfonso-Corcuera D, Álvarez J M, Cubas J and Pindado S 2020 Lambert w-function simplified expressions for photovoltaic current-voltage modelling *2020 IEEE International Conference on Environment and Electrical Engineering and 2020 IEEE Industrial and Commercial Power Systems Europe (EEEIC / I CPS Europe)* pp 1–6

[16] Pindado S, Cubas J, Roibás-Millán E and Sorribes-Palmer F 2018 *CEAS Space Journal* **10** 307–323

[17] Pindado S, Cubas J, Roibás-Millán E, Bugallo-Siegel F and Sorribes-Palmer F 2018 *Energies* **11** ISSN 1996-1073 URL https://www.mdpi.com/1996-1073/11/6/1353

[18] Pindado S and Cubas J 2017 *Renewable Energy* **103** 729–738 ISSN 0960-1481 URL https://www.sciencedirect.com/science/article/pii/S0960148116309697

[19] Roibás-Millán E, Alonso-Moragón A, Jiménez-Mateos A and Pindado S 2017 *Measurement Science and Technology* **28** 115801

[20] Cubas J, Pindado S and De Manuel C 2014 *Energies* **7** 4098–4115 ISSN 1996-1073 URL https://www.mdpi.com/1996-1073/7/7/4098

[21] Cubas J, Pindado S and Victoria M 2014 *Journal of Power Sources* **247** 467–474 ISSN 0378-7753 URL https://www.sciencedirect.com/science/article/pii/S0378775313014997

[22] Cubas J, Pindado S and Farrahi A 2013 New method for analytical photovoltaic parameter extraction *2013 International Conference on Renewable Energy Research and Applications (ICRERA)* pp 873–877

[23] RECOM Switching Regulator DC-DC converters https://docs.rs-online.com/9296/0900766b812daffc.pdf

[24] Lithium-Ion Rechargeable Cell Model: INR18650-29E https://eu.nkon.nl/sk/k/29E.pdf

[25] IPS-3303 D.C. Power Supply https://docs.rs-online.com/2ce7/0900766b8156d900.pdf

[26] Digital Multimeter PD-181 https://www.promax.es/downloads/manuals/2Lang/PD-181.pdf

[27] Mayuno DC Electronic Load M9812 http://www.maynuo.com/english/pro.asp?tid=98

[28] Porras-Hermoso, A and Pindado, S and Cubas, J 2018 *Measurement Science and Technology* **29** 117002 URL https://doi.org/10.1088/1361-6501/aae231

[29] IT8500+ Programmable DC Electronic Load https://www.itechate.com/en/info_128.aspx?lcid=14&itemid=99

[30] BK PRECISION 8500 Programmable Electronic Load https://www.bkprecision.com/products/dc-electronic-loads/8500B-8500b-300-w-programmable-dc-electronic-load.html